Electrostatic solitary structures in a dusty plasma with dust of opposite polarity

A. A. Mamun
Department of Physics, Jahangirnagar University, Savar, Dhaka-1342, Bangladesh
(Received 15 September 2007; published 12 February 2008)

A four-component dusty plasma consisting of electrons, ions, positively charged warm adiabatic dust, and negatively charged cold dust is considered. The basic features of the electrostatic solitary structures in such a four-component dusty plasma are investigated by the reductive perturbation method, which is valid for the small amplitude solitary waves, and by the pseudopotential approach which is valid for the arbitrary amplitude solitary waves. It is found that the presence of the positive dust component does not only significantly modify the basic properties of the solitary potential structures, but also causes the coexistence of the positive and negative solitary potential structures, which is an interesting feature shown in a dusty plasma with the dust of opposite polarity. The basic features and the underlying physics of the electrostatic solitary structures, which are relevant to cometary tails, upper mesosphere, Jupiter's magnetosphere, etc., are briefly discussed.

DOI: 10.1103/PhysRevE.77.026406 PACS number(s): 52.27.Lw, 94.05.Bf

I. INTRODUCTION

The physics of charged dust, which are ubiquitous in space plasmas, has received a great deal of interest in understanding the electrostatic density perturbations and solitary potential structures that are observed in different regions of space, viz. mesosphere, cometary tails, planetary rings, planetary magnetospheres, interplanetary space, interstellar media, etc. [1–5]. The electrostatic density perturbations and solitary potential structures observed in such different regions of space have been theoretically investigated by considering a most commonly used dusty plasma model [6–14] that assumes electrons, ions, and negatively charged dust.

Rao *et al.* [6] and Mamun [11] considered negatively charged mobile dust with Boltzmann electrons and ions, and studied the basic features of the dust-acoustic (DA) solitary waves by employing the reductive perturbation method [6] and the pseudopotential approach [11]. The effects of the dust charge fluctuation [8,9], vortexlike ion distribution [10], nonplanar geometry [12], and dust-neutral collisions [13] on the basic features of the DA solitary waves have been investigated. Xue [14] has investigated the interaction of two DA solitary waves in an unmagnetized dusty plasma containing negatively charged dust, electrons, and ions. On the other hand, Bharuthram and Shukla [7] have considered negatively charged static dust with mobile ions and Boltzmann electrons, and studied the dust ion-acoustic solitary waves.

The presence of positively charged dust has also been observed in different regions of space, viz. cometary tails [3,15], upper mesosphere [16], Jupiter's magnetosphere [3,17], etc. There are three principal mechanisms by which dust grains become positively charged [18]. These are (i) photoemission in the presence of a flux of ultraviolet photons, (ii) thermionic emission induced by the radiative heating, and (iii) secondary emission of electrons from the surface of the dust grains. Chow *et al.* [19] have theoretically shown that due to the size effect on secondary emission, insulating dust grains of different sizes can have the opposite polarity (smaller ones being positive and larger ones being negative). This is mainly due to the fact that the excited secondary electrons have shorter (longer) distances to travel to reach the surface of the smaller (larger) dust grains [19].

There is also direct evidence for the existence of both positive and negative dust in different regions of space, viz. cometary tails [3,15], upper mesosphere [16], Jupiter's magnetosphere [3,17], etc. Recently, based on these theoretical predictions and satellite observations, Mamun and Shukla [20] have considered a very simple dusty plasma model, which assumes positive and negative dust only, and have theoretically investigated the properties of linear and nonlinear electrostatic waves in such a dusty plasma. The simple dusty plasma model of Mamun and Shukla [20] is only valid if a complete depletion of the background electrons and ions is possible, and both positive and negative dust fluids are cold. However, in most space dusty plasma systems a complete depletion of the background electrons and ions is not possible [5,21], and the positive dust component is of finite temperature. The present work is therefore attempted to generalize the model of Mamun and Shukla [20] to a more realistic space dusty plasma situation, which is particularly relevant to cometary tails [3,15], upper mesosphere [16], and Jupiter's magnetosphere [3,17], by considering a four-component dusty plasma containing negatively charged cold dust (of larger size), positively charged warm adiabatic dust (of smaller size), and Boltzmann electrons and ions. It is found that the presence of the positive dust component does not only significantly modify the basic properties of the solitary potential structures, but also causes the coexistence of the positive and negative solitary potential structures in such a dusty plasma.

The paper is organized as follows. The basic equations governing the dusty plasma system under consideration are given in Sec. II. The properties of the small amplitude (SA) electrostatic solitary potential structures are investigated in Sec. III, and those of the arbitrary amplitude (AA) ones are examined in Sec. IV. A brief discussion is presented in Sec. V.

II. GOVERNING EQUATIONS

We consider an unmagnetized four-component dusty plasma system consisting of negatively charged cold dust,

positively charged warm adiabatic dust, and Boltzmann electrons and ions. We assume that the negative dust grains are much more massive than the positive ones. This model is relevant to dusty plasmas in cometary tails [3,15], upper mesosphere [16], and Jupiter's magnetosphere [3,17], where dust is charged by the secondary emission or photoemission or thermionic emission, and the dust size effect on the latter is important. The dynamics of the one dimensional DA waves [5,6,11] in such a dusty plasma system is governed by

$$\frac{\partial N_1}{\partial t} + \frac{\partial}{\partial x}(N_1 U_1) = 0, \tag{1}$$

$$\frac{\partial U_1}{\partial t} + U_1 \frac{\partial U_1}{\partial x} = \frac{\partial \Psi}{\partial x}, \tag{2}$$

$$\frac{\partial N_2}{\partial t} + \frac{\partial}{\partial x}(N_2 U_2) = 0, \tag{3}$$

$$\frac{\partial U_2}{\partial t} + U_2 \frac{\partial U_2}{\partial x} = -\alpha\left(\frac{\partial \Psi}{\partial x} + \frac{\sigma_d}{N_2}\frac{\partial P_2}{\partial x}\right), \tag{4}$$

$$\frac{\partial P_2}{\partial t} + U_2 \frac{\partial P_2}{\partial x} + 3P_2 \frac{\partial U_2}{\partial x} = 0, \tag{5}$$

$$\frac{\partial^2 \Psi}{\partial x^2} = N_1 - \mu_2 N_2 + \mu_e e^{\sigma\Psi} - \mu_i e^{-\Psi}, \tag{6}$$

where N_1 (N_2) is the negative (positive) dust number density normalized by its equilibrium value n_{10} (n_{20}), U_1 (U_2) is the negative (positive) dust fluid speed normalized by $C_1 = (Z_1 k_B T_i/m_1)^{1/2}$, Ψ is the wave potential normalized by $k_B T_i/e$, $\alpha = Z_2 m_1/Z_1 m_2$, P_2 is the thermal pressure of the positive dust fluid normalized by its equilibrium value $n_{20} k_B T_d$, $\sigma_d = T_d/Z_2 T_i$, $\mu_e = n_{e0}/Z_1 n_{10}$, $\mu_i = n_{i0}/Z_1 n_{10}$, $\mu_2 = 1 + \mu_e - \mu_i$, $\sigma = T_i/T_e$, Z_1 (Z_2) is the number of electrons (protons) residing on a negative (positive) dust, m_1 (m_2) is the mass of the negative (positive) dust particle, T_i (T_e) is the ion (electron) temperature, T_d is the temperature of the positive dust fluid, k_B is the Boltzmann constant, and $-e$ is the electronic charge. The time variable t is normalized by $\omega_{p1}^{-1} = (m_1/4\pi Z_1^2 e^2 n_{10})^{1/2}$, and the space variable x is normalized by $\lambda_D = (Z_1 k_B T_i/4\pi Z_1^2 e^2 n_{10})^{1/2}$. It should be mentioned here that the effects of the dust charge fluctuation [22] have been neglected since the dust charging time (few microseconds) is much less than the time period (a fraction of a second) of the low-frequency DA waves under consideration [5].

III. SA SOLITARY WAVES

We first investigate the basic features of the small amplitude (SA) electrostatic solitary waves by the reductive perturbation technique, and the stretched coordinates [23] $\zeta = \epsilon^{1/2}(x - V_0 t)$, $\tau = \epsilon^{3/2} t$, where ϵ is a small parameter measuring the weakness of the dispersion, and V_0 is the phase speed normalized by C_1. The variables N_1, U_1, N_2, U_2, P_2, and Ψ can be expanded in power series of ϵ as

$$N_1 = 1 + \epsilon N_1^{(1)} + \epsilon^2 N_1^{(2)} + \cdots, \tag{7}$$

$$U_1 = 0 + \epsilon U_1^{(1)} + \epsilon^2 U_1^{(2)} + \cdots, \tag{8}$$

$$N_2 = 1 + \epsilon N_2^{(1)} + \epsilon^2 N_2^{(2)} + \cdots, \tag{9}$$

$$U_2 = 0 + \epsilon U_2^{(1)} + \epsilon^2 U_2^{(2)} + \cdots, \tag{10}$$

$$P_2 = 1 + \epsilon P_2^{(1)} + \epsilon^2 P_2^{(2)} + \cdots, \tag{11}$$

$$\Psi = 0 + \epsilon \Psi^{(1)} + \epsilon^2 \Psi^{(2)} + \cdots. \tag{12}$$

Now, expressing Eqs. (1)–(6) in terms of ζ and τ, and substituting Eqs. (7)–(12) into the resulting equations [Eqs. (1)–(6) expressed in terms of ζ and τ], one can easily develop different sets of equations in various powers of ϵ. To the lowest order in ϵ one obtains

$$N_1^{(1)} = \frac{U_1^{(1)}}{V_0} = -\frac{\Psi^{(1)}}{V_0^2}, \tag{13}$$

$$N_2^{(1)} = \frac{U_2^{(1)}}{V_0} = \frac{\alpha \Psi^{(1)}}{V_0^2 \sigma_\alpha}, \tag{14}$$

$$P_2^{(1)} = \frac{3\alpha \Psi^{(1)}}{V_0^2 \sigma_\alpha}, \tag{15}$$

$$V_0^2 = \frac{1 + \alpha\mu_2 + \sigma_\mu}{2(\mu_i + \mu_e \sigma)}(1 + \sigma_p), \tag{16}$$

where $\sigma_\alpha = 1 - 3\alpha\sigma_d/V_0^2$, $\sigma_\mu = \alpha\sigma_d(\mu_i + \mu_e\sigma)$, and $\sigma_p = [1 - 12\alpha\sigma_d/(1 + \alpha\mu_2 + \sigma_\mu)^2]^{1/2}$. Equation (16) is the linear dispersion relation for the DA waves propagating in a dusty plasma under consideration. Similarly, to the next order in ϵ, one gets another set of equations which, after using Eqs. (13)–(16), can be reduced to a Korteweg–de Vries (KdV) equation,

$$\frac{\partial \Psi^{(1)}}{\partial \tau} + A\Psi^{(1)}\frac{\partial \Psi^{(1)}}{\partial \zeta} + B\frac{\partial^3 \Psi^{(1)}}{\partial \zeta^3} = 0, \tag{17}$$

where the coefficients A and B are given by

$$A = B\left[\mu_i - \sigma^2 \mu_e - \frac{3}{V_0^4}(1 - \alpha^2 \mu_2 \sigma_\nu)\right], \tag{18}$$

$$B = \frac{V_0^3 \sigma_\alpha^2}{2(\sigma_\alpha^2 + \alpha\mu_2)}, \tag{19}$$

and $\sigma_\nu = (1 + \alpha\sigma_d/V_0^2)/\sigma_\alpha^3$. Now, transforming the independent variables ζ and τ to $\xi = \zeta - U_0\tau'$ and $\tau = \tau'$ (where U_0 is a constant speed normalized by C_1), and imposing the appropriate boundary conditions (viz. $\Psi^{(1)} \to 0$, $\partial\Psi^{(1)}/\partial\xi \to 0$, $\partial^2\Psi^{(1)}/\partial\xi^2 \to 0$ at $\xi \to \pm\infty$), one can express the stationary solitary wave solution of the KdV Eq. (17) as

$$\Psi^{(1)} = \Psi_m \,\mathrm{sech}^2(\xi/\Delta), \tag{20}$$

where the amplitude Ψ_m (normalized by $k_B T_i/e$) and the width Δ (normalized by λ_D) are given by

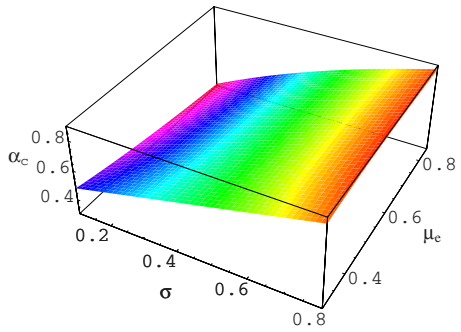

FIG. 1. (Color online) Showing how α_c [obtained from $A(\alpha=\alpha_c)=0$] varies with σ and μ_e for $\mu_i=0.6$ and $\sigma_d=0.001$.

$$\Psi_m = \frac{3U_0}{A}, \tag{21}$$

$$\Delta = \sqrt{4B/U_0}. \tag{22}$$

It is obvious from Eqs. (20)–(22) that as U_0 increases, the amplitude (width) of the solitary waves increases (decreases). It is clear from Eqs. (18), (20), and (21) that the solitary potential profile is positive (negative) if $A>0$ ($A<0$). Therefore $A(\alpha=\alpha_c)=0$, where α_c is the critical value of α above (below) which the solitary waves with a positive (negative) potential exists gives the value of α_c. To find the parametric regimes for which the positive and negative solitary potential profiles exist, we have numerically analyzed A, and obtain $A(\alpha=\alpha_c)=0$ surface plots. The $A(\alpha=\alpha_c)=0$ surface plots are shown in Figs. 1 and 2. It is clear from Eq. (21) that $\Psi_m=\infty$ at $\alpha=\alpha_c$. This means that the small amplitude solitary waves with a negative (positive) potential exist for a set of dusty plasma parameters corresponding to any point which is much below (above) the $A(\alpha=\alpha_c)=0$ surfaces shown in Figs. 1 and 2. Figures 1 and 2 show that α_c, which is a function of σ, σ_d, μ_e, and μ_i, increases with the increase of σ, μ_e, and μ_i for a constant σ_d. Therefore for typical dusty plasma parameters, viz. $\sigma_d=0.001$, $\sigma=0.1-0.9$, $\mu_e=0.2-0.9$, and $\mu_i=0.3-0.9$, we have the existence of the small amplitude solitary waves with a negative potential for $\alpha=0.095<\alpha_c$, and with a positive potential for $\alpha=1.495>\alpha_c$.

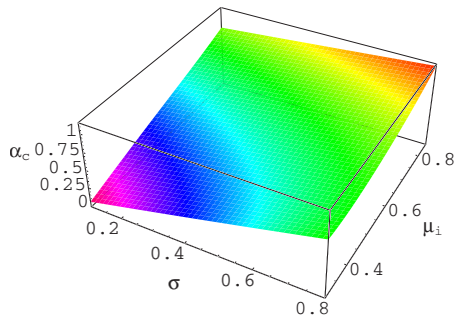

FIG. 2. (Color online) Showing how α_c [obtained from $A(\alpha=\alpha_c)=0$] varies with σ and μ_i for $\mu_e=0.3$ and $\sigma_d=0.001$.

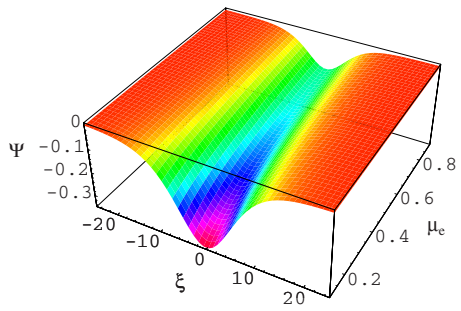

FIG. 3. (Color online) Showing how the amplitude and the width of the negative solitary potential profiles vary with μ_e for $\mu_i=0.6$, $\sigma=0.5$, $\alpha=0.1$, $\sigma_d=0.001$, $U_0=V_0$, and $\epsilon=0.05$.

To examine the basic properties (amplitude and width) of the small amplitude electrostatic solitary structures, the solitary profiles of $\Psi \simeq \epsilon\Psi^{(1)}$ are graphically shown. These are displayed in Figs. 3–8. It is obvious from Figs. 3–5 that the magnitude of the amplitude and the width of the negative solitary potential profiles decrease with the increase of μ_e, μ_i, and σ. On the other hand, it is seen from Figs. 6–8 that the amplitude of the positive solitary potential profiles increases with the increase of μ_e, μ_i, and σ, but their width decreases with the increase of μ_e, μ_i, and σ. One can easily check by such a numerical analysis that the effect of σ_d on these basic features of the DA solitary waves is not significant (in comparison with that of μ_e, μ_i, and σ). However, analyzing the variation of Ψ_m and Δ with only σ_d (keeping the other parameters constant), one can show that as σ_d is increased, the amplitude (Ψ_m) decreases, but the width (Δ) increases. It may be noted here that if one sets $\sigma_d=0$, and, instead of the combined effects of these parameters, one analyzes the effects of any single parameter (keeping the other parameters constant) on these features of the DA solitary waves, these results completely agree with the work of Sayed and Mamun [21] which is valid only for the small amplitude solitary waves, but not for the arbitrary amplitude (AA) solitary waves.

IV. AA SOLITARY WAVES

To study the arbitrary amplitude solitary waves, we employ the pseudopotential approach [24] by assuming that all

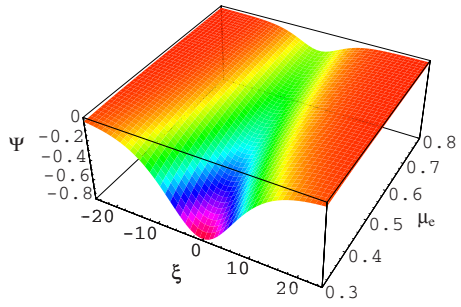

FIG. 4. (Color online) Showing how the amplitude and the width of the negative solitary potential profiles vary with μ_i for $\mu_e=0.2$, $\sigma=0.5$, $\alpha=0.1$, $\sigma_d=0.001$, $U_0=V_0$, and $\epsilon=0.05$.

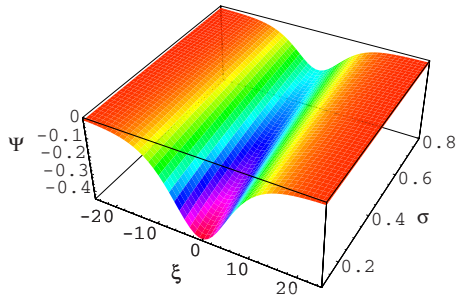

FIG. 5. (Color online) Showing how the amplitude and the width of the negative solitary potential profiles vary with σ for $\mu_e=0.2$, $\mu_i=0.6$, $\alpha=0.1$, $\sigma_d=0.001$, $U_0=V_0$, and $\epsilon=0.05$.

dependent variables depend on a single variable $\xi=x-Mt$, where M is the Mach number. This transformation ($\xi=x-Mt$) along with the steady state condition ($\partial/\partial t=0$) allows us to write Eqs. (1)–(6) as

$$M\frac{\partial N_1}{\partial \xi}-\frac{\partial}{\partial \xi}(N_1U_1)=0, \tag{23}$$

$$M\frac{\partial U_1}{\partial \xi}-U_1\frac{\partial U_1}{\partial \xi}=-\frac{\partial \Psi}{\partial \xi}, \tag{24}$$

$$M\frac{\partial N_2}{\partial \xi}-\frac{\partial}{\partial \xi}(N_2U_2)=0, \tag{25}$$

$$M\frac{\partial U_2}{\partial \xi}-U_2\frac{\partial U_2}{\partial \xi}=\alpha\left(\frac{\partial \Psi}{\partial \xi}+\frac{\sigma_d}{N_2}\frac{\partial P_2}{\partial \xi}\right), \tag{26}$$

$$M\frac{\partial P_2}{\partial \xi}-U_2\frac{\partial P_2}{\partial \xi}-3P_2\frac{\partial U_2}{\partial \xi}=0, \tag{27}$$

$$\frac{\partial^2 \Psi}{\partial \xi^2}=N_1-\mu_2N_2+\mu_e e^{\sigma\Psi}-\mu_i e^{-\Psi}. \tag{28}$$

Now, using Eqs. (23)–(26) and applying the appropriate boundary conditions for localized perturbations (viz. $N_1\to 1$, $N_2\to 1$, $U_1\to 0$, $U_2\to 0$, $P_2\to 1$, and $\Psi\to 0$ at $\xi\to\pm\infty$), one can express N_1 and N_2 as

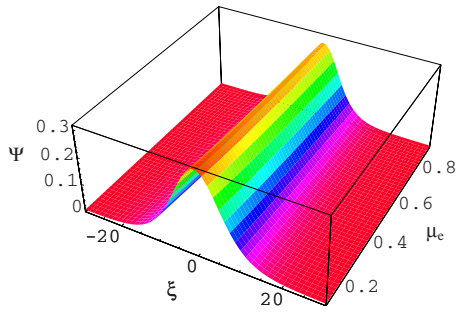

FIG. 6. (Color online) Showing how the amplitude and the width of the positive solitary potential profiles vary with μ_e for $\mu_i=0.6$, $\sigma=0.5$, $\alpha=1.5$, $\sigma_d=0.001$, $U_0=V_0$, and $\epsilon=0.05$.

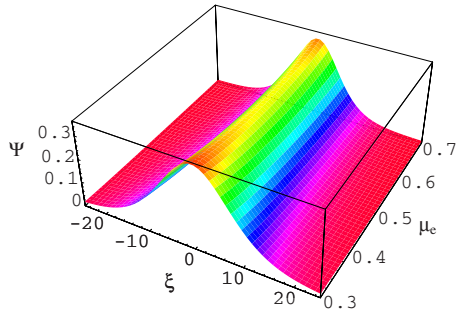

FIG. 7. (Color online) Showing how the amplitude and the width of the positive solitary potential profiles vary with μ_i for $\mu_e=0.2$, $\sigma=0.5$, $\alpha=1.5$, $\sigma_d=0.001$, $U_0=V_0$, and $\epsilon=0.05$.

$$N_1=\left(1+\frac{2\Psi}{M^2}\right)^{-1/2}, \tag{29}$$

$$N_2=\frac{M_\beta}{\sqrt{6\alpha\sigma_d}}(\Psi_1-\Psi_2)^{1/2}, \tag{30}$$

where $\Psi_1=1-2\alpha\Psi/M_\beta^2$, $\Psi_2=(\Psi_1^2-12\alpha\sigma_d M^2/M_\beta^4)^{1/2}$, and $M_\beta=(M^2+3\alpha\sigma_d)^{1/2}$. We note that Eq. (30) is obtained from $3\alpha\sigma_d N_2^4-(M_\beta^2-2\alpha\Psi)N_2^2+M^2=0$ which reduces to $N_2=(1-2\alpha\Psi/M^2)^{-1/2}$ for $\sigma_d=0$. Now, substituting Eqs. (29) and (30) into Eq. (28), multiplying the resulting equation by $d\Psi/d\xi$, and applying the boundary condition, $d\Phi/d\xi\to 0$ at $\xi\to\pm\infty$, one obtains

$$\frac{1}{2}\left(\frac{d\Psi}{d\xi}\right)^2+V(\Psi)=0, \tag{31}$$

where $V(\Psi)$ is given by

$$V(\Psi)=-\frac{\mu_e}{\sigma}e^{\sigma\Psi}-\mu_i e^{-\Psi}-M^2\left(1+\frac{2\Psi}{M^2}\right)^{1/2}-\frac{\mu_2 M M_\beta}{\alpha\sqrt{2}}(\Psi_1+\Psi_2)^{1/2}-2^{3/2}\sigma_d\frac{\mu_2 M^3}{M_\beta^3}(\Psi_1+\Psi_2)^{-3/2}+C, \tag{32}$$

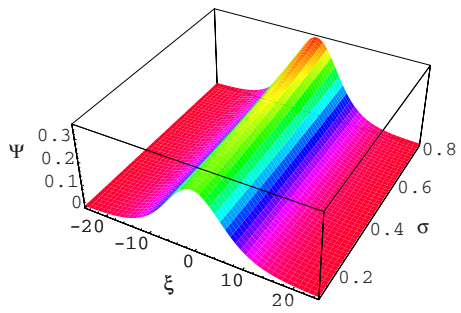

FIG. 8. (Color online) Showing how the amplitude and the width of the positive solitary potential profiles vary with σ for $\mu_e=0.2$, $\mu_i=0.6$, $\alpha=1.5$, $\sigma_d=0.001$, $U_0=V_0$, and $\epsilon=0.05$.

in which C is the integration constant and is chosen in such a way that $V(\Psi)=0$ at $\Psi=0$. Equation (31) can be regarded as an "energy integral" of an oscillating particle of unit mass, with pseudospeed $d\Psi/d\xi$, pseudoposition Ψ, pseudotime ξ, and pseudopotential $V(\Psi)$.

The expansion of $V(\Psi)$ around $\Psi=0$ is

$$V(\Psi) = C_2\Psi^2 + C_3\Psi^3 + \cdots, \tag{33}$$

where

$$C_2 = -\frac{1}{2}\left[\mu_i + \sigma\mu_e - \frac{1}{M^2}\left(1 + \frac{\alpha\mu_2}{\sigma_o}\right)\right], \tag{34}$$

$$C_3 = \frac{1}{6}\left[\mu_i - \sigma^2\mu_e - \frac{3}{M^4}(1 - \alpha^2\mu_2\sigma_c)\right], \tag{35}$$

in which $\sigma_c=(1+\alpha\sigma_d/M^2)/\sigma_o^3$ and $\sigma_o=1-3\alpha\sigma_d/M^2$. To compare the basic features of the solitary structures obtained from the reductive perturbation method [23] with those obtained from this pseudopotential approach [24], let us first consider small amplitude solitary waves for which $V(\Psi)=C_2\Psi^2+C_3\Psi^3$ holds good. This approximation allows us to write the small amplitude solitary wave solution of Eq. (31) as

$$\Psi = \left(-\frac{C_2}{C_3}\right)\mathrm{sech}^2\left(\sqrt{-\frac{C_2}{4}}\xi\right). \tag{36}$$

This means that when $C_2<0$, the small amplitude solitary waves with a positive (negative) potential exist for $(C_3>0)$ $(C_3<0)$. So, $C_2(M=M_c)=0$, where M_c is the critical value of M above which the solitary wave solutions exist, gives the value of M_c:

$$M_c^2 = \frac{1+\alpha\mu_2+\sigma_\mu}{2(\mu_i+\mu_e\sigma)}(1+\sigma_p), \tag{37}$$

and $C_3(M=M_c,\alpha=\alpha_c)=0$ gives the value of α_c. It is obvious from Eqs. (16), (18), (35), and (37) that $V_0=M_c$ and that $A(\alpha=\alpha_c)=0$ and $C_3(M=M_c,\alpha=\alpha_c)=0$ yield exactly the same expression for α_c. The variation of α_c [obtained from $C_3(M=M_c,\alpha=\alpha_c)=0$ or $A(\alpha=\alpha_c)=0$] with different dusty plasma parameters is shown in Figs. 1 and 2, which show that α_c increases with the increase of σ, μ_e, and μ_i, and the variation of M_c or V_0 with different dusty plasma parameters is shown in Figs. 9 and 10, which show that M_c increases with the increase of α and μ_e, but decreases with the increase of σ and μ_i. Therefore the basic features of these small amplitude solitary structures identified by the pseudopotential approach [24] are identical to those identified by the reductive perturbation method [23].

We now study the nature of the arbitrary amplitude solitary waves by analyzing the general expression for $V(\Psi)$ [Eq. (32) or Eq. (33)]. It is clear from Eq. (33) that $V(\Psi)=dV(\Psi)/d\Psi=0$ at $\Psi=0$. Therefore the solitary wave solutions of Eq. (31) exist [25,26] if (i) $(d^2V/d\Psi^2)_{\Psi=0}<0$ so that the fixed point at the origin is unstable, and (ii) $(d^3V/d\Psi^3)_{\Psi=0}>(<)0$ for the solitary waves with $\Psi>(<)0$. Condition (i) is satisfied when $C_2<0$, i.e., $M>M_c$, and condition (ii) is satisfied when $C_3(M=M_c)>(<)0$, i.e., $\alpha<(>)\alpha_c$ for the solitary waves with $\Psi<(>)0$. To make it more clear, we consider typical dusty plasma parameters, namely, $\sigma=0.5$, $\sigma_d=0.001$, $\mu_e=0.2$, and $\mu_i=0.8$. It is obvious from Figs. 1 and 2 that for this particular set of dusty plasma parameters $\alpha_c\simeq 0.995$. Therefore for this particular set of dusty plasma parameters, we have the existence of the arbitrary amplitude solitary waves with a negative potential for $\alpha=0.5<\alpha_c$ and $M>M_c\simeq 1.195$, and the coexistence of the arbitrary amplitude solitary waves with a positive potential for $\alpha=1.5>\alpha_c$ and $M>M_c\simeq 1.4095$. We have verified this result by the numerical analysis of Eq. (32), and found that for any set of dusty plasma parameters satisfying $M>M_c$ and $\alpha<\alpha_c$, the potential wells are formed in the negative Ψ axis only, i.e., the solitary waves exist with $\Psi<0$ only, and that for any set of dusty plasma parameters satisfying $M>M_c$ and $\alpha>\alpha_c$, the potential wells are formed in both the positive and negative Ψ axes, i.e., the solitary waves with $\Psi<0$ and $\Psi>0$ coexist. One can also verify by this numerical analysis that as σ_d is increased, the amplitude Ψ_m [the nonzero value of Ψ for which $V(\Psi_m)=0$] of the DA solitary waves decreases. It has been shown as an example that for typical dusty plasma parameters, viz. $\sigma=0.5$, $\sigma_d=0.001$, $\mu_e=0.2$, and $\mu_i=0.8$, the solitary waves with a negative potentials exist for $\alpha=0.5<\alpha_c$ and $M>M_c\simeq 1.2$ (as clearly shown in Fig. 11), and the solitary waves with negative and positive potential coexist for $\alpha=1.5>\alpha_c$ and $M>M_c\simeq 1.4095$ (as clearly shown Figs. 12 and 13). It may be noted here that one cannot show the potential wells on

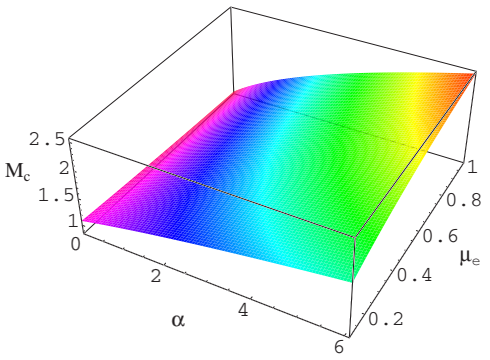

FIG. 9. (Color online) Showing how M_c varies with α and μ_e for $\sigma=0.5$, $\sigma_d=0.001$, and $\mu_i=0.8$.

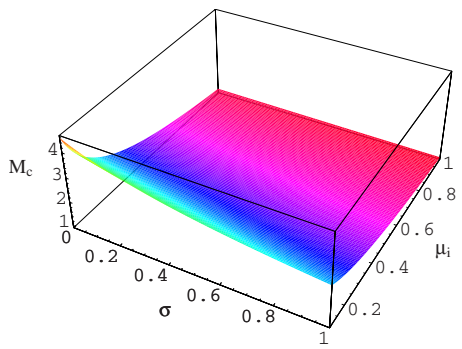

FIG. 10. (Color online) Showing how M_c varies with σ and μ_i for $\alpha=1$, $\sigma_d=0.001$, and $\mu_e=0.2$.

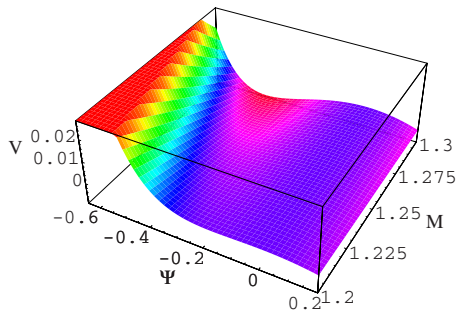

FIG. 11. (Color online) Showing the formation of the potential wells in the negative Ψ axis when M exceeds the value of M_c which is 1.195 for $\alpha=0.5$, $\sigma=0.5$, $\sigma_d=0.001$, $\mu_e=0.2$, and $\mu_i=0.8$. We note that no potential well is formed in the positive Ψ axis for any values of α, σ, σ_d, μ_e, and μ_i lying below the $C_3(M=M_c, \alpha=\alpha_c)=0$ surfaces. This means that in this case the negative solitary potential structures can only exist.

both the positive and negative Ψ axes in a single surface plot clearly, since for the same set of parameters [lying above the $C_3(M=M_c, \alpha=\alpha_c)=0$ surfaces] the potential wells formed in the negative Ψ axis are very deep in comparison with those formed in the positive Ψ axis. It should be kept in mind for the numerical analysis of $V(\Psi)$ that $-M<2\Psi<M_\beta^2(1-M\sqrt{12\alpha\sigma_d}/M_\beta^2)/\alpha$ must be valid in order to have real values of N_1 and N_2.

V. DISCUSSION

The basic features of the DA solitary waves in an unmagnetized dusty plasma containing the dust of opposite polarity (cold negative dust and warm adiabatic positive dust) and Boltzmann electrons and ions are investigated theoretically. The results, which have been found from this investigation, can be summarized as follows.

We have found that the presence of the positive (second) dust component causes the existence of the positive solitary potential profile. It is important to mention that if one neglects the presence of the positive (second) dust component, i.e., $\alpha=0$, one finds that the nonlinear coefficient A of the KdV equation is always negative. This means that the negative solitary potential profile can only exist. This completely agrees with Mamun [11].

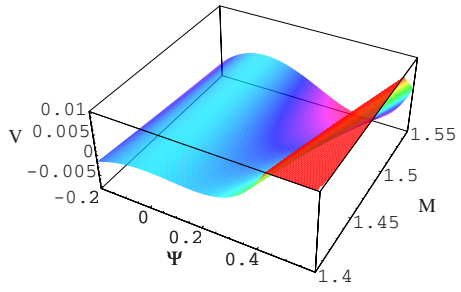

FIG. 12. (Color online) Showing the formation of the potential wells in the positive Ψ axis when M exceeds the value of M_c which is 1.405 for $\alpha=1.5$, $\sigma=0.5$, $\sigma_d=0.001$, $\mu_e=0.2$, and $\mu_i=0.8$. This means that the solitary waves with a positive potential exist.

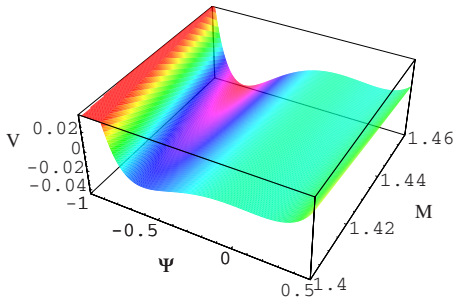

FIG. 13. (Color online) Showing the formation of the deeper potential wells in the negative Ψ axis when M exceeds the value of M_c which is 1.405 for $\alpha=1.5$, $\sigma=0.5$, $\sigma_d=0.001$, $\mu_e=0.2$, and $\mu_i=0.8$. This means that the solitary waves with a negative potential exist. It may be noted here that the parameters used here are exactly the same as those used in Fig. 12.

It has been found for the small amplitude limit that (i) the magnitude of the amplitude of the negative solitary profiles and their width decreases with increasing the values of μ_e, μ_i, and σ (as is clearly shown in Figs. 3–5); (ii) the amplitude of the positive solitary potential profiles increases with μ_e, μ_i, and σ (as is clearly shown in Figs. 6–8); (iii) the width of both the negative and positive solitary profiles decreases with μ_e, μ_i, and σ (as is clearly shown in Figs. 6–8); (iv) the speed of the small amplitude solitary waves increases with the increase of α and μ (as is clearly shown in Fig. 9), but decreases with the increase of σ and μ_i (as is clearly shown in Fig. 10).

To study the properties of the arbitrary amplitude electrostatic solitary potential by the pseudopotential approach, it has been found that the critical Mach number (M_c) for the existence of the arbitrary amplitude solitary potential structures increases with α and μ (as is clearly shown in Fig. 9), but decreases with σ and μ_i (as is clearly shown in Fig. 10). The parametric regimes [corresponding to any point above the $C_3(M=M_c, \alpha=\alpha_c)=0$ surface plots, clearly shown in Figs. 1 and 2] for the coexistence of the arbitrary amplitude positive and negative solitary potential structures are obtained (as is clearly shown in Figs. 12 and 13). It has been found that the presence of the positive dust component does not only significantly modify the basic properties of the electrostatic solitary potential structures, but also causes the coexistence of the positive and negative solitary potential structures (as is clearly shown in Figs. 12 and 13), which is an interesting feature shown in a dusty plasma with the dust of opposite polarity.

The ranges ($\sigma=0.1-0.9$, $\mu_e=0.2-0.9$, and $\mu_i=0.3-0.9$) of the dusty plasma parameters used in this numerical analysis are very wide. Therefore the dusty plasma parameters (viz. σ, μ_e, and μ_i) corresponding to cometary tails [3,15], upper mesosphere [16], and Jupiter's magnetosphere [3,17] are, certainly, within these ranges (viz. $\sigma=0.1-0.9$, $\mu_e=0.2-0.9$, and $\mu_i=0.3-0.9$). The values of α and σ_d, for which the existence of the solitary waves is found, are also within the ranges of the dusty plasma parameters corresponding to cometary tails [3,15], upper mesosphere [16],

and Jupiter's magnetosphere [3,17]. It ought to be stressed that the solitary negative (positive) potential may trap positive (negative) dust, which, in turn, attract dust of opposite polarity to form larger sized dust or to be coagulated into extremely large sized neutral dust in cometary tails, upper mesosphere, Jupiter's magnetosphere, or even in laboratory experiments. Therefore the present investigation can help us to identify the origin of charge separation as well as dust coagulation in a plasma containing positive and negative dust. It can be expected that the basic features and the underlying physics of the DA solitary waves that have been presented in the present work should be verified by further laboratory experiments. It may therefore be proposed to perform a laboratory experiment which will be able to identify the special features of the DA solitary waves that have been predicted in this investigation.

ACKNOWLEDGMENTS

The author acknowledges the suggestions of Professor P. K. Shukla and the financial support of the Jahangirnagar University during the course of this work.

[1] C. K. Goertz, Rev. Geophys. **27**, 271 (1989).
[2] D. A. Mendis and M. Rosenberg, Annu. Rev. Astron. Astrophys. **32**, 419 (1994).
[3] M. Horányi, Annu. Rev. Astron. Astrophys. **34**, 383 (1996).
[4] F. Verheest, *Waves in Dusty Plasmas* (Kluwer Academic Publishers, Dordrecht, 2000).
[5] P. K. Shukla and A. A. Mamun, *Introduction to Dusty Plasma Physics* (IoP Publishing Ltd., Bristol, 2002), pp. 8–27.
[6] N. N. Rao, P. K. Shukla, and M. Y. Yu, Planet. Space Sci. **38**, 543 (1990).
[7] R. Bharuthram and P. K. Shukla, Planet. Space Sci. **40**, 973 (1992).
[8] J. X. Ma and J. Liu, Phys. Plasmas **4**, 253 (1997).
[9] M. R. Gupta, S. Sarkar, S. Ghosh, M. Debnath, and M. Khan, Phys. Rev. E **63**, 046406 (2001).
[10] A. A. Mamun, Phys. Scr. **57**, 258 (1998).
[11] A. A. Mamun, Astrophys. Space Sci. **268**, 443 (1999).
[12] A. A. Mamun and P. K. Shukla, Phys. Lett. A **290**, 173 (2001).
[13] W. M. Moslem, Phys. Plasmas **10**, 3168 (2003).
[14] Ju-Kui Xue, Phys. Rev. E **69**, 016403 (2004).
[15] D. A. Mendis and M. Horányi, in *Comentary Plasma Processes*, Geophysics Monograph Series No. 61, edited by A. D. Johnstone (AGU, Washington, DC, 1991), p. 17.
[16] O. Havnes *et al.*, J. Geophys. Res. **101**, 10839 (1996).
[17] M. Horányi, G. E. Morfill, and E. Grün, Nature (London) **363**, 144 (1993).
[18] V. E. Fortov *et al.*, J. Exp. Theor. Phys. **87**, 1087 (1998) [Zh. Eksp. Teor. Fiz. **114**, 2004 (1998)].
[19] V. W. Chow, D. A. Mendis, and M. Rosenberg, J. Geophys. Res. **98**, 19065 (1993).
[20] A. A. Mamun and P. K. Shukla, Geophys. Res. Lett. **29**, 1870 (2002).
[21] F. Sayed and A. A. Mamun, Phys. Plasmas **14**, 014501 (2007).
[22] R. K. Varma, P. K. Shukla, and V. Krishan, Phys. Rev. E **47**, 3612 (1993).
[23] H. Washimi and T. Taniuti, Phys. Rev. Lett. **17**, 996 (1966).
[24] I. B. Bernstein, J. M. Greene, and M. D. Kruskal, Phys. Rev. **108**, 546 (1957).
[25] R. A. Cairns *et al.*, Geophys. Res. Lett. **22**, 2709 (1995).
[26] A. A. Mamun, Phys. Rev. E **55**, 1852 (1997).